frontiers in Energy Research

ORIGINAL RESEARCH
published: 11 October 2019
doi: 10.3389/fenrg.2019.00107

CO_2 Hydrogenation Induced by Mechanochemical Activation of Olivine With Water Under CO_2 Atmosphere

Valeria Farina[1], Nadia S. Gamba[2], Fabiana Gennari[2], Sebastiano Garroni[1], Francesco Torre[3], Alessandro Taras[1], Stefano Enzo[1] and Gabriele Mulas[1]**

[1] Dipartimento di Chimica e Farmacia, Università degli Studi di Sassari and INSTM, Sassari, Italy, [2] Departamento Fisicoquímica de Materiales, Gerencia de Investigación Aplicada, Centro Atómico Bariloche (CNEA) y Consejo Nacional de Investigaciones Científicas y Técnicas (CONICET), San Carlos de Bariloche, Argentina, [3] Dipartimento di Ingegneria Meccanica, Chimica e dei Materiali, Università degli Studi di Cagliari, Cagliari, Italy

OPEN ACCESS

Edited by:
José Carlos Netto-Ferreira, Universidade Federal Rural do Rio de Janeiro, Brazil

Reviewed by:
Rafael Mattos Dos Santos, University of Guelph, Canada
Alicja M. Lacinska, British Geological Survey (BGS), United Kingdom

***Correspondence:**
Valeria Farina
vfarina1@uniss.it
Gabriele Mulas
mulas@uniss.it

Specialty section:
This article was submitted to Carbon Capture, Storage, and Utilization, a section of the journal Frontiers in Energy Research

Received: *15 April 2019*
Accepted: *20 September 2019*
Published: *11 October 2019*

Citation:
Farina V, Gamba NS, Gennari F, Garroni S, Torre F, Taras A, Enzo S and Mulas G (2019) CO_2 Hydrogenation Induced by Mechanochemical Activation of Olivine With Water Under CO_2 Atmosphere. Front. Energy Res. 7:107. doi: 10.3389/fenrg.2019.00107

A study on the mechanochemical activation of the olivine in presence of H_2O and under CO_2 atmosphere have been approached, focusing both on the structural nature of the transformation and the conversion of CO_2 to methane and light hydrocarbons. The mechanochemical process was carried out by high energy laboratory mills, with milling vials properly modified in order to be used as batch reactors. Chemical reactivity and reaction rates were investigated under different experimental conditions, evidencing increased performance with respect to the thermally activated process reported in literature. Mechanical treatment induced H_2O and olivine activation, with consequent release of molecular H_2 which, in turn, allowed hydrogenation of activated CO_2. This last reaction also led, through a competitive process, to the precipitation of carbonate phases, whose composition and structural features were dependent of the CO_2/H_2O ratio.

Keywords: CO_2 utilization, olivine, methane, mechanochemical activation, hydrogen

INTRODUCTION

Fossil fuels are still the primary energy source in the world. However, the energy demand, in continuous growth, has led to increased fuel consumption and then to the release of a huge amount of carbon dioxide, CO_2, into the atmosphere (Koukouzas et al., 2009). It is well-known that CO_2 is the greenhouse gas with the major contribution to global warming. It is also recognized that natural processes cannot absorb all the anthropogenically produced carbon dioxide. As a consequence, the development of new technologies for capture and conversion is urgently required (Falkowski et al., 2000).

Global emissions of CO_2 have been increasing steadily in the past decades and reached values 60% above 1990 levels, when the Kyoto Protocol was stated. In order to limit the global temperature rise, CO_2 emissions should be reduced by at least 50% by 2050 (Stocker et al., 2014; Cuéllar-Franca and Azapagic, 2015).

Among the various strategies under investigation, Carbon Capture Storage (CCS) and, more recently Carbon Capture Utilization (CCU), have attracted the attention of scientists worldwide. The aim of such approaches is to capture emissions from point sources but the main difference is

the destination of captured CO_2. While in CCS it is transferred to a suitable site for long-term storage, in CCU it is converted into valuable products (e.g., chemicals and fuels), contributing to mitigate climate change (Metz et al., 2005; Weisser, 2007; Hertwich et al., 2008; Cooper, 2009; Nagashima et al., 2011; Styring and Jansen, 2011; Markewitz et al., 2012; Zapp et al., 2012).

As for the CCS, i.e., CO_2 geological storage, it involves the injection of CO_2 into geological formations, such as depleted oil and gas reservoirs at great depths. Such sequestration technique is, at present, probably one of the most promising options due to the previous experience by the oil and gas industry. In fact, the industry has a good understanding of the structural characteristics and behavior of depleted oil and gas reservoirs, and the existing well-drilling and injection techniques can be adapted for carbon storage applications (Metz et al., 2005) (e.g., CO_2-injection at Sleipner) (Leung et al., 2014; Furre et al., 2017). The main issues with CO_2 storage are their possible leaks and the related damage that would cause if a concentrated stream escaped into the environment. This possibility depends on the permeability of the geological structure and its faults or defects. According to the literature, annual leakage rates are in the range from 0.00001 to 1% (Metz et al., 2005; Pehnt and Henkel, 2009; Singh et al., 2011).

Finally, mineral carbonation, also known as "mineral sequestration," can be considered as a storage and utilization option, because it involves CO_2 conversion into carbonates through the reaction with metal oxides, such as magnesium or calcium oxide (Metz et al., 2005; Von Der Assen et al., 2013). The carbonation is an exothermic reaction that releases enough heat to make the whole carbonation process, at least in theory, self-sustaining (Von Der Assen et al., 2013). The main advantage of mineral carbonation is the formation of stable carbonates capable of storing CO_2 for long periods, without the risk of CO_2 leakage as in CCS (Metz et al., 2005; Styring and Jansen, 2011; Von Der Assen et al., 2013).

Olivine and Serpentine minerals are the most promising candidates for carbon sequestration because of their high contents of magnesium. The main carbonation reactions of these two minerals are described by the following reactions (Equations 1–3):

$$(Mg,Fe)_2SiO_4 + 2CO_2 \rightarrow 2(Mg,Fe)CO_3 + SiO_2 \quad (1)$$

$$6(Mg,Fe)_2SiO_4 + 12H_2O + 6CO_2 \rightarrow 2(Mg,Fe)_3Si_2O_5(OH)_4 + 2Fe_3O_4 + 8H_2 + 6MgCO_3 + 2SiO_2 \quad (2)$$

$$(Mg,Fe)_3Si_2O_5(OH)_4 + 3CO_2 \rightarrow 3(Mg,Fe)CO_3 + 2SiO_2 + 2H_2O \quad (3)$$

In nature, around 100 million tons of carbon per year, according to a slow weathering process, is bound by these minerals (Oelkers et al., 2008). The CO_2 sequestration in natural silicates is sometimes accompanied by the occurrence of the serpentinization process. This is a widespread phenomenon on the Earth's mantle that occurs generally at temperatures $<300°C$ (Oelkers et al., 2008; McCollom and Bach, 2009; Neubeck et al., 2011; Holm et al., 2015), and during which, mineral based silicates of Fe and Mg react with water to give H_2 and minerals of the serpentine group [$(Mg,Fe)_3Si_2O_5(OH)_4$] (Equation 2). This involves the formation of extremely reducing fluids, rich in hydrogen, so any species present, such as inorganic C, can be reduced. Therefore, CO_2 can react with H_2, through a Fischer-Tropsch type (FTT) or Sabatier mechanism, to form CH_4 and light hydrocarbons (Holm et al., 2015) (Equation 4).

$$CO_2 + 4H_2 \rightarrow CH_4 + 2H_2O \quad (4)$$

Although the whole process is thermodynamically favored, the rate of the reaction is very slow, and, accordingly, the natural process does not allow control of CO_2 emission levels into the atmosphere. The possibility to increase the kinetics of such processes deserves interest, and to this regard, preliminary treatment of the olivine mineral, such as mechanical activation, has been demonstrated to be successful. If, on the one hand, the CO_2 absorption process during olivine serpentinization had been experimentally investigated, on the other hand, literature data (Kleiv and Thornhill, 2006; Baláž et al., 2008; Fabian et al., 2010; Sandvik et al., 2011; Power et al., 2013; Turianicová et al., 2013; Li and Hitch, 2015; Rigopoulos et al., 2015) are not homogeneous and refer to the effects of mechanical activation on olivine, focusing mainly on its structural and surface transformation, in order to facilitate CO_2 storage. In particular, it has been shown that the mechanical grinding of olivine significantly increases its ability to form iron and magnesium carbonates making the CO_2 capture a potential stable storage method for long periods. The mechanical activation was found to be more effective if the treatment occurs in the presence of liquids, such as water (Turianicová and Baláz, 2008) or ethanol (Rigopoulos et al., 2015), as a consequence of the greater surface area generated in wet conditions. Conversely, less attention has been paid, in such studies, to the chemical reduction of CO_2, to yield light hydrocarbons and corresponding oxygenated compounds. The present work just deals with such issues, and, for the first time to the best of our knowledge, the attention has been focused on the mechanically induced production of methane and light hydrocarbons during the interaction between olivine and water under CO_2 atmosphere.

MATERIALS AND METHODS

Olivine powders were provided by SATEF-HA (Italy). Chemical analysis reported by the supplier indicated the following relative composition expressed as weight % of oxide of each element contained in the material: 50.00% MgO, 41.50% SiO_2, 7.30% Fe_2O_3, 0.29% Cr_2O_3, 0.40% Al_2O_3, 0.30% NiO, 0.10% MnO, 0.10% CaO.

High purity Carbon dioxide gas ($\geq$99.995%) was provided by Sapio (Italy).

Materials Processing

The mechanical activation was carried out by a Spex Mixer Mill mod.8000, which was suitably modified to control the milling dynamic parameters (Delogu et al., 2004).

As a mechanochemical reactor, we employed a stainless-steel vial (76 cm^3) equipped with two circular bases which were

fitted with sealing valves. On one side, these valves allowed the connection to the gas reservoir (CO_2), and on the other side, to the GC apparatus for the analyses of gaseous reagents and products. The mechanical treatments were carried out on fresh powders at selected milling times. In order to remove the residual air from the vial, a dynamic vacuum of 10^{-3} mbar for 10 min was applied, before introducing CO_2. Gas sampling was then performing 30 min after stopping milling and the gases analyzed by gas chromatography.

Three series of experiments have been performed by charging the vial with 2 g of olivine, 0.3 ml of deionized H_2O, three stainless steel balls of 3.80 g each, and a rotation speed of 875 rpm. The reactor was then closed under CO_2 atmosphere under different conditions: (a) applying a constant pressure of 1.5 bar; (b) pressurizing the milling vial with an initial pressure of 1.5 bar; (c) filling the reactor with 1.0 bar. All the mechanochemical processes were conducted under low pressure of CO_2, in order to reproduce the reaction conditions expected under a real environment.

Methane, Hydrogen, and Light Hydrocarbons Evolution

Gas withdrawal from the reactor and injection in the gas sampling valves of gas chromatographs (GC) were performed by a gastight syringe. A GC Perkin Elmer 8600 equipped with a capillary column (GSQ 115-3432-J&W Scientific) and an FID detector, was used for CH_4 and light hydrocarbons detection. A Fisons 8000 equipped with a molecular sieves column (10 Å) and a hot wire detector (HWD), was used to evaluate H_2 and permanent gases. The conversion of CO_2, expressed as percentage (%), was calculated using the following equation:

$$CO_2\ conversion\ (\%) = \frac{CO_{2initial} - CO_{2final}}{CO_{2initial}} * 100 \qquad (5)$$

where $CO_{2initial}$ and CO_{2final} correspond to the area of the peak showed by GC measurements before and after the mechanical treatment, respectively.

Quantitative analyses were carried out through calibration curves setup by resorting to analytical standards, provided by Linde Gas Italia S.R.L.

Solid-State Samples Characterization

Powders were structurally characterized by means of a Rigaku SmartLab X-ray Diffractometer (XRD) with a Bragg–Brentano geometry using Cu Kα radiation (λ = 1.54178 Å) and a graphite monochromator in the diffracted beam. Quantitative evaluation of phase abundance and structural features were obtained for all the XRD patterns, by non-linear least-square refinement procedure, according to Rietveld method, and using the MAUD (Materials Analysis Using Diffraction) software (Young, 1993).

The thermogravimetric analyses were carried out by a Setaram Labsys DTA-TGA under Argon flux, by heating the specimens from room temperature to 1,000°C, at a scanning rate equal to 5°C/min.

RESULTS

The crystallographic characterization of the olivine powders in the as-received state was performed by XRD using the Rietveld refinement method (**Figure 1**). In this way, phases were identified and their relative abundance and microstructural features were evaluated (**Table 1**). The Mg-rich Olivine used in these tests (from now Olivine) consists of three phases: Forsterite ($Fe_{0.2}Mg_{1.8}SiO_4$), space group (s.g.) Pbnm, Enstatite ferroan ($Fe_{0.2}Mg_{0.8}SiO_3$), s.g. Pbca, and Clinochlore ($Al_{1.84}Fe_{0.5}H_8Mg_{4.5}O_{18}Si_{3.16}$), s.g. C-1. The Forsterite is the majority phase in the as-received olivine powders (91 wt%), with Enstatite as secondary phase (7.5 wt%).

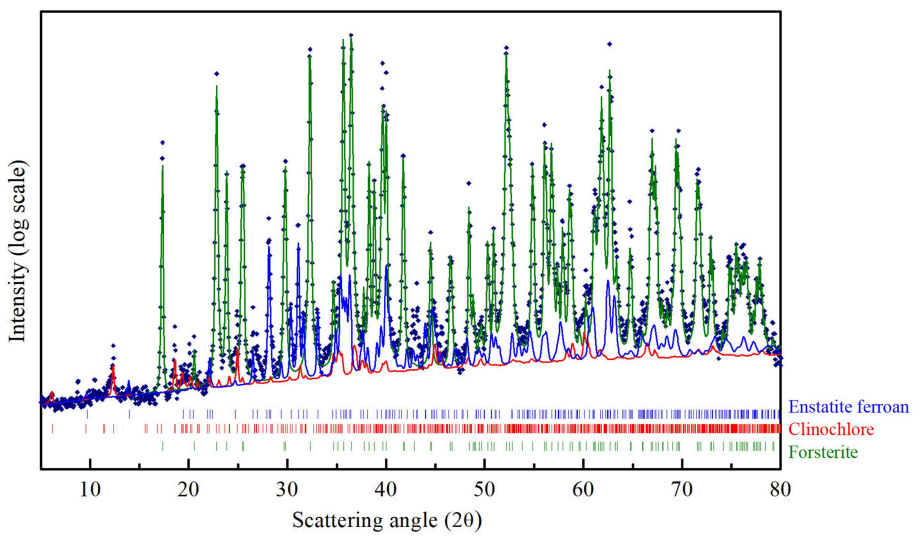

FIGURE 1 | CuKα XRD pattern of the Olivine in the as received state. The structural refinement procedure by Rietveld method, allowed to quantitatively evaluate the contribution of the three phases indicated in the Figure: Forsterite (green line), Enstatite ferroan (blue line), Clinochlore (red trace).

TABLE 1 | Phase composition and structural parameters of Olivine in the as-received state.

Phases	a (Å)	b (Å)	c (Å)	α (°)	β (°)	γ (°)	r.m.s. (%)*	Wt (%)
Forsterite	4.77	10.23	5.99	–	–	–	0.0000021	90.8
Clinochlore	5.31	9.23	14.39	90.76	96.68	89.63	0.00523	1.7
Enstatite ferroan	18.24	8.83	5.19	–	–	–	0.00119	7.5

**Root mean square microstrain.*
*All data were obtained by Rietveld analysis on the pattern reported in **Figure 1**, using MAUD software.*

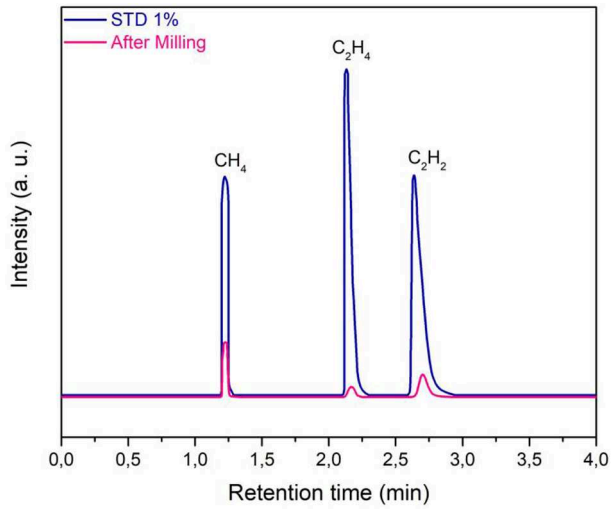

FIGURE 2 | Gas-chromatographic analysis, by FID, of the gas phase sampled from the mechanochemical reactor. Experimental data, reported as pink line, are compared with the relevant standard mixture data (STD), relative to 1% concentration value.

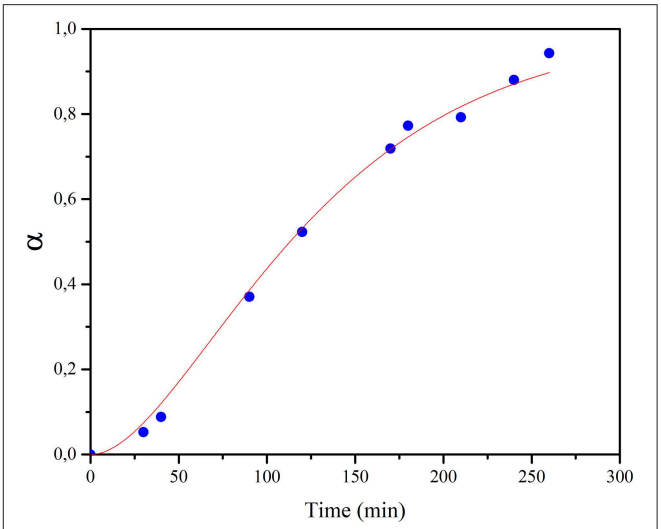

FIGURE 3 | Methane concentration values in the gas phase mixture, reported as degree of conversion α, as a function of mechanical treatment time, *t*. Blue dots refer to experimental data, while continuous line represents the fitting curve according to the empirical equation reported in the text.

As a general behavior, mechanical activation tests of olivine with water under CO_2 atmosphere led to the production of different gas-phase products, which were detected by gas chromatography. The main hydrocarbons produced were methane, CH_4, ethane, C_2H_6, and ethylene, C_2H_4. As an example, the gas-chromatographic trace of olivine mechanically treated for 150 min is shown (**Figure 2**). The relative concentration of light hydrocarbons and other gas phase compounds, within the mechanochemical reactor, was evaluated by a calibration line obtained using certificated standard gas mixtures. Data plotted in **Figure 2** indicate that the relative amount is: 0.23% v/v of methane, 0.036% v/v of ethane, and 0.099% v/v of ethylene. Moreover, it is safe to say that, at present, we cannot exclude the formation of traces of further heavier products, which could be in condensed liquid phase, or chemisorbed on the powder surfaces: this point is still under investigation. However, concerning the present work, we focused our attention mainly on the formation of methane. It should also be noted that, in absence of CO_2, there was no methane formation, during two blank tests carried out by filling the jar with air or Argon.

The evolution of methane during the experiments performed under a constant pressure of 1.5 bar of CO_2 (with continuous flow) is presented in **Figure 3**. Data are reported in the graph as a degree of conversion α, vs. the milling time. The kinetics of evolution of methane concentration followed a sigmoidal shape, a trend often observed in chemical reactions involving solids as well as in gas-solid interaction processes, also activated by mechanical treatment (Delogu et al., 2004; Ahmedabadi and Kain, 2019). The data suggest that methane formation rate, initially slow ($\alpha = 8.3 \cdot 10^{-3}$), increased up to reaching its maximum value after about 150 min of milling, and then CO_2 to CH_4 conversion progressively slows down, asymptotically approaching $\alpha = 1$, which corresponds to the CH_4 maximum concentration value, between 0.18 and 0.2% v/v. Experimental points can be fitted by the empirical equation $\alpha = 1 - (1 + kt)\, exp\,(-kt)$, in which t represents the milling time, and k represents the apparent kinetic constant of the process and has a value of $1.484^{*}10^{-2}$ min^{-1}. Apart from the empirical approach, it should be noted that the actual process is rather complex, as it involves several steps, including surface adsorption of H_2O and CO_2, with molecular dissociation occurring over the surface, or after diffusion phenomena through the bulk. Such steps are accompanied by the creation of highly activated and freshly renewed surfaces due to the milling process, corresponding to sites where CO_2 conversion can take place. Despite the complexity of the process, which makes it difficult to reliably define the different reaction steps, some hints can be obtained by analyzing the experimental results, as described below.

In order to evaluate structural and microstructural changes of the olivine during mechanical activation, XRD analyses were performed (**Figure 4**). A decrease in the crystallite size of the predominant Forsterite phase due to the milling process

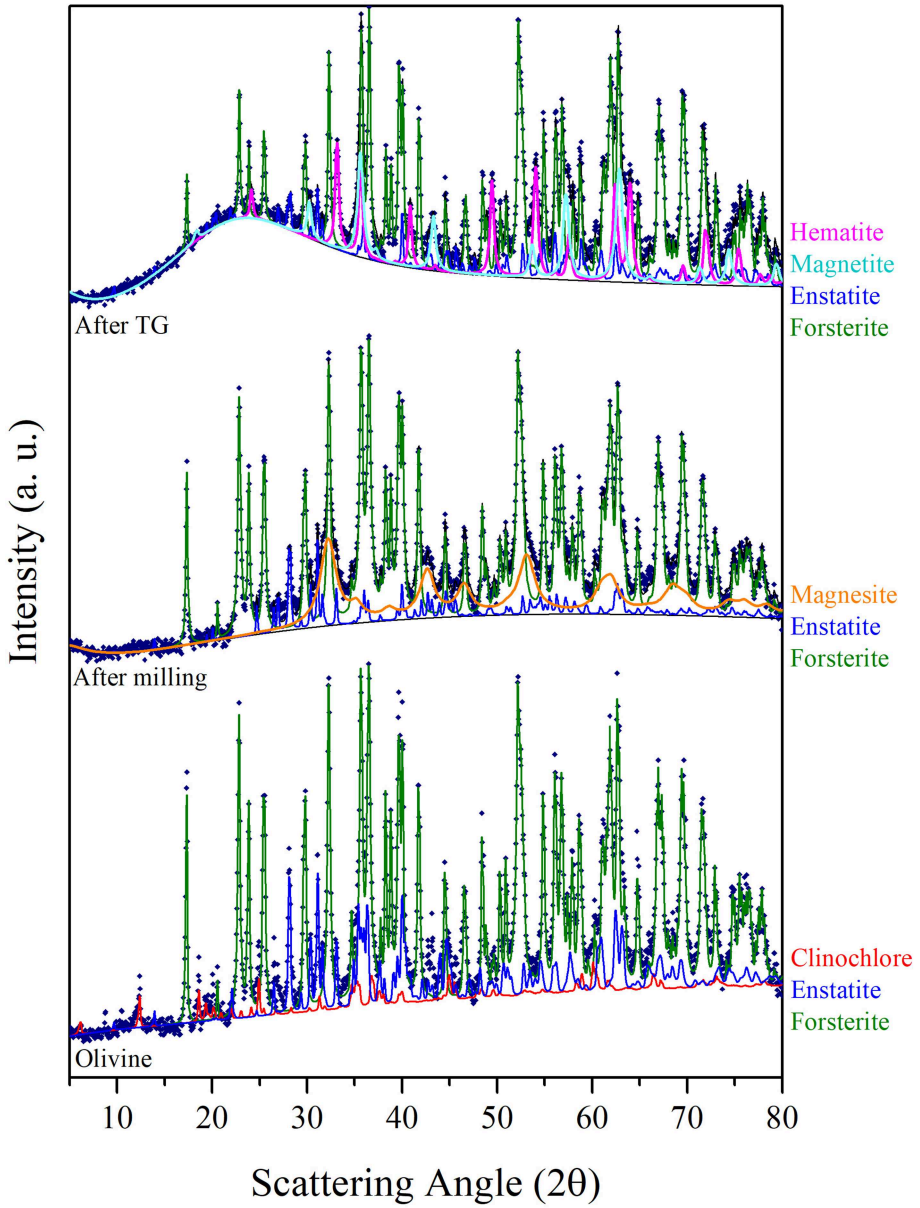

FIGURE 4 | The CuKα XRD patterns sequence displays, from the bottom, the analyses of the Olivine in the as received state, the one of the sample at the end of 90 min of mechanical activation in the first series of runs, and the one further subjected to the thermogravimetric analysis. Experimental points are fitted by the Rietveld refinement procedure.

was obtained by Rietveld refinement (**Table 2**). XRD patterns presented in **Figure 4** do not evidence the formation of a Serpentine phase. However, these patterns display, together with the residual Forsterite, the formation of two Mg-based phases, which can be identified as the trigonal $MgCO_3$, Magnesite, s.g. R-3C, and the orthorhombic $MgSiO_3$, Enstatite, s.g. Pbca. Such phases were observed in all the samples at the end of the mechanochemical trials, as displayed in **Table 3**. An example is the XRD pattern of the olivine subjected to 90 min of mechanochemical activation (central trace of **Figure 4**). The data suggest that the transformation process of olivine was accompanied by CO_2 adsorption on the mineral surface, and further activation, which induces the formation of Magnesium carbonates phases. No Fe-based carbonates were detected. However, after heat treatment up to 1,000°C of this as-activated olivine (upper trace of **Figure 4**), the precipitation of two crystalline Fe-oxide phases, namely Hematite Fe_2O_3, s.g. R-3C, and Magnetite Fe_3O_4, s.g. Fd-3m was observed.

Figure 5 shows the TGA curves of the pristine olivine and the samples previously subject to different milling times.

Whereas, for pristine olivine, which did not display significant changes in weight, all the other TG curves are characterized by two weight loss phenomena, occurring within three main temperature ranges (20–100, 100–400, and 400–1,000°C). The comparison with literature data suggests that the weight loss occurring at lower temperature ranges is related to H_2O desorption by the sample surface (Maroto-Valer et al., 2005); the subsequent signal, whose onset is observable at about 107°C can be related to the dehydration of the bulk; the last weight loss (around 450°C) can be conversely related to CO_2 evolution after decomposition of carbonate phases (Bisbal et al., 2015; Stopic et al., 2018). It can, thus, be argued that the heat treatment allowed H_2O and CO_2 evolution from these compounds, and that the decomposition of $MgCO_3$ (Magnesite) induced the increase of $MgSiO_3$ concentration (Enstatite) up to about 8%. The precipitation and grain growth of Hematite and Magnetite phases, whose relative amount are reported in **Table 3**, deserve further analysis.

It is noteworthy that the above findings are in agreement with Klein (2014) and Jones et al. (2010) who reported the treatment of olivine with H_2O and CO_2, under hydrothermal conditions, at low-temperatures and in presence of an excess CO_3^{2-} ions. In that case, Fe^{2+} ions were rapidly incorporated to form carbonates, silicates and hydroxides, rather than being oxidized to Fe^{3+}, and can also be included within the serpentine, thus not leading to the precipitation of appreciable amounts of Magnetite. According to this, it could be surmised that, in our tests, the Magnesite carbonate phase, that formed as a consequence of mechanical activation of olivine with H_2O and CO_2, is not a pure Mg^{2+} based phase, but includes Fe ions. This is confirmed by crystallographic features: values of lattice parameters *a* and *c* of the R-3C carbonate phase, equal to 4,682 and 15,218 Å, respectively, are consistent with a ca. equimolecular mixture of the two Fe- and Mg-carbonate phases whose corresponding lattice parameters are $a = 4{,}686$ Å, $c = 15{,}383$ Å, and $a = 4{,}635$ Å, $c = 15{,}023$ Å, respectively.

The driving force of the serpentinization process lies in the oxidation of Fe^{2+} to Fe^{3+} that leads to the reduction of water and the formation of molecular hydrogen. As a matter of fact, the whole analysis of gaseous mixture, from the mechanochemical reactor at the end of tests, allowed for confirmation of the occurrence of a significant amount of gaseous H_2. This hydrogen appeared due to H_2O activation and dissociation, and it was made available, within the vial, as a consequence of its desorption from powders. Its kinetic trend parallels the shape of CO_2 to CH_4 transformation (**Figure 6**), and its value is relevant to samples mechanically treated up to 150 min, which show that the H_2 concentration rises up to about 20% v/v. Assuming 1 atm pressure inside the vial, the amounts of H_2 detected are stoichiometrically possible (54% of the theoretical maximum) based on the available Fe^{2+} amount. The CO_2 conversion (**Figure 7**) shows that the kinetic trend recalls that observed for H_2: the increasing rate has to be considered as the initial step of a sigmoid-shaped curve, while the observed conversion values indicate, on one hand, the efficiency of the mechanochemical process as a tool for CO_2 storage, and on the other hand, confirm that CO_2 absorption and activation steps are necessary conditions that precede the reduction to form methane.

In order to evaluate the effect of the CO_2 pressure, as registered within the milling vial, on the transformation path

TABLE 2 | Crystallite size of the Forsterite phase, evaluated by Rietveld analysis of each sample, as a function of the milling time.

Milling time (min)	Forsterite crystallite size (nm)
0	230
30	92
90	85
180	82
240	76

TABLE 3 | Phase composition, as evaluated by Rietveld analysis, of different samples after selected time of mechanical treatment, in the first series of tests.

Sample	Phases (Wt%)						
	Forsterite $Fe_{0.2}Mg_{1.8}SiO_4$ **orthorhombic**	***Clinochlore*** $Al_{1.84}Fe_{0.5}H_8Mg_{4.5}O_{18}Si_{3.16}$ **triclinic**	***Enstatite ferroan*** $Fe_{0.155}Mg_{0.845}SiO_3$ **orthorhombic**	***Enstatite*** $MgSiO_3$ **orthorhombic**	***Magnesite*** $MgCO_3$ **trigonal**	***Hematite*** Fe_2O_3 **trigonal**	***Magnetite*** Fe_3O_4 **cubic**
Olivina AR	90.8%	1.7%	7.5%				
30 min	79%			2.9%	18.1%		
After TG	82.9%			8.1%		5.9%	3.1%
90 min	85.1%			2.8%	12.1%		
After TG	80.1%			7.6%		7%	5.3%
180 min	80.6%			2.8%	16.6%		
After TG	78.6%			5.8%		8.9%	6.6%
240 min	79.9%			2.5%	17.6%		
After TG	77.1%			7.6%		11.6%	3.7%

Constant pressure of 1.5 bar of CO_2 (AR, as received; TG, thermogravimetric measurement up to 1,000°C).

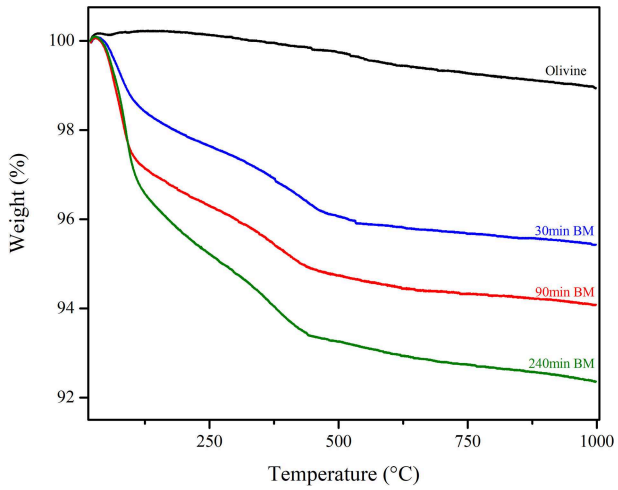

FIGURE 5 | TGA traces carried out over selected samples at the end of the first series runs, i.e., mechanochemical tests carried out under a CO_2 pressure head equal to 1.5 bar.

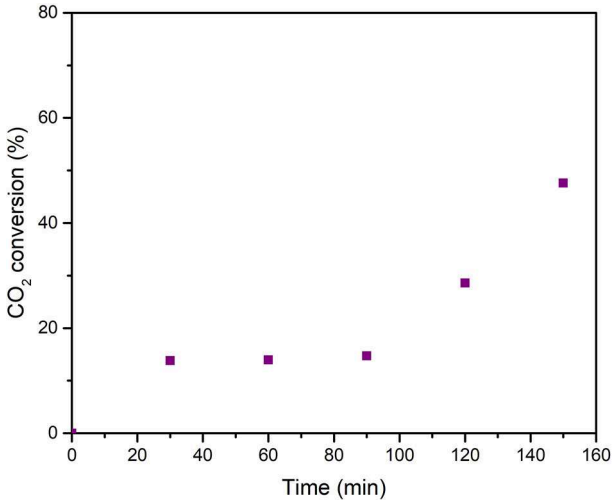

FIGURE 7 | Conversion data of CO_2, plotted as a function of milling time, as observed during the series of mechanochemical tests performed with a pressure head of 1.5 bar of CO_2.

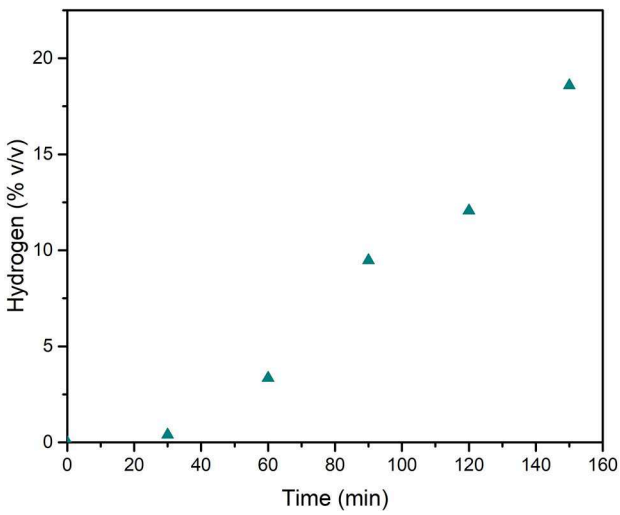

FIGURE 6 | H_2 concentration in the gas phase within the mechanochemical reactor, as registered at different times of mechanical treatment, in the tests carried out with a pressure head of 1.5 bar of CO_2.

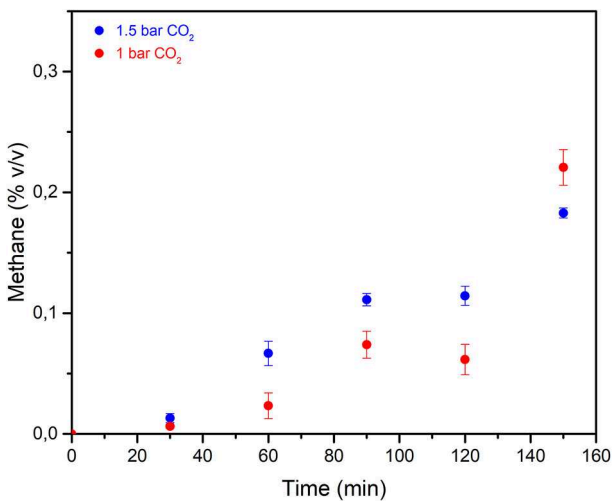

FIGURE 8 | Methane concentration data relevant to the three different test series. Blue dots: initial CO_2 pressure equal to 1.5 bar. Red dots: initial CO_2 pressure equal to 1.0 bar. The data are replicates of two runs and error bars refers to standard deviation values.

under mechanochemical activation, two subsequent series of tests were carried out by changing the value of the CO_2/H_2O ratio, by setting the CO_2 initial pressure of the vial at 1.5 bar and at 1.0 bar, respectively.

The CH_4 concentration values reported in **Figure 8** correspond to the above series of experiments. It emerged that CO_2 conversion trend, as well as the H_2 evolution, approach the results of formerly presented runs at corresponding times of mechanical treatment. The data of the two series have similar trends and are in the same order of magnitude, with a small increase observed in the tests carried out at an initial pressure equal to 1.5 bar. For samples milled for 120 min, the lower conversion value marks a difference in the rising trend, and it parallels the corresponding data for H_2 evolution at the same time of treatment. Although the amount of gaseous H_2 available within the vial remains much higher than the stoichiometric requirement for the hydrogenation process, the dependence of the conversion on the H_2/CO_2 ratio may be a relevant factor.

As for the solid phases, a difference in the evolution of the phases was evidenced by XRD data (**Table 3**), which refer to the first series of tests performed under constant CO_2 pressure value equal to 1.5 bar. These results revealed the formation of the Mg-carbonate phase, the trigonal $Mg(CO_3)$, Magnesite, s.g. R-3C, while no relevant signals of Nesquehonite were observed.

TABLE 4 | Phase composition, as evaluated by Rietveld analysis, of different samples after selected time of mechanical treatment, in the second series of tests, run under the initial CO_2 pressure of 1 bar.

Sample	Phases (Wt%)							
	Forsterite $Fe_{0.184}Mg_{1.816}SiO_4$ orthorhombic	*Clinochlore* $Al_{1.84}Fe_{0.5}H_8Mg_{4.5}O_{18}Si_{3.16}$ triclinic	*Enstatite ferroan* $Fe_{0.155}Mg_{0.845}SiO_3$ orthorhombic	*Enstatite* $MgSiO_3$ orthorhombic	*Magnesite* $MgCO_3$ trigonal	*Nesquehonite* $Mg(CO_3)\cdot 3H_2O$ monoclinic	*Hematite* Fe_2O_3 trigonal	*Magnetite* Fe_3O_4 cubic
Olivina AR	90.8%	1.7%	7.5%					
30 min	89.8%	2%		8.2%				
After TG	86.6%			8.1%			4.3%	1%
60 min	84.1%	2.8%		9.5%		3.7%		
After TG	83.9%			6.5%			7.1%	2.5%
90 min	84.4%	3.8%		6.8%		5.5%		
After TG	84.2%			6.4%			6.6%	2.7%
120 min	86.5%	3.8%		3.1%		6.6%		
After TG	83.2%			5.6%			8.6%	2.6%
150 min	83.6%			2.9%	13.5%			
After TG	80.2%			5.2%			11.9%	2.7%

Different finding was observed in the third series of tests (carried out at initial CO_2 pressure of 1 bar) the Nesquehonite phase appeared in all the samples except for the one milled for 150 min, and it is consistent with the reduced value of the CO_2/H_2O ratio (**Table 4**). This suggests the sensibility of the chemical transformation to the adopted conditions. In this regard, it is interesting to note that our findings agree with the literature data, referred to the process in a liquid medium, which indicate that the precipitation of Magnesite at room temperature is not observed, despite being the stable carbonate form. Most commonly, only the Nesquehonite mineral can precipitate from aqueous solution at 25°C and with a partial pressure of CO_2 close to ambient pressure. At higher temperatures, above 40°C, several basic carbonates were observed to precipitate, in the form of hydromagnesite. Conversely, Magnesite production takes place only if the temperature is around 60–100°, and at high CO_2 pressure (Fernández et al., 2000; Zhang et al., 2000; Kloprogge et al., 2003; Giammar et al., 2005; Hänchen et al., 2008).

A further point deserves a comment: the Clinochlore phase, observed in the above tests, was present in a low amount (about 1.7 wt%) in the as-received Olivine and it was not found in the first series of experiments, where the mixed carbonate, Magnesite-type, was recovered. However, its content increased in the other series, where hydrated Nesquehonite compound was formed. In other words, during the process, decreasing the CO_2/H_2O ratio, the concentration of the resulting carbonate form decreases, and under such conditions, the formed carbonate phase is hydrated. Therefore, the absence in XRD data of the signals, related to the Serpentine, at the end of the mechanochemical runs, could be related to a possible phase amorphization during the process. A further possible interpretation is the occurrence of a consecutive process. The former step is related to olivine hydrolysis, with the induced formation of Serpentine minerals, which still evolve, in the latter step, to give carbonates when CO_2 is available in the proper amount. Otherwise, in the tests carried out with a lower value of CO_2/H_2O ratio, the kinetics of the latter step slows down, allowing to observe the rise of the Clinochlore phase concentration.

Finally it is noteworthy that Magnetite, reported as the active catalytic phase *in situ* generated during FTT after olivine hydrolysis under hydrothermal conditions (Giammar et al., 2005; Jones et al., 2010), was not observed during our mechanochemical runs, but only after thermal annealing at TGA. However, it is safe to say that, under mechanochemical activation, a necessary condition for the occurrence of FTT after olivine weathering process, is the presence of Fe^{3+} ions more than actual Magnetite particles.

CONCLUSIONS

The mineral carbonation technology is capturing wide interest as a useful strategy for both CO_2 storage and its utilization, and in this context, the chemical transformations driven by olivine weathering process appear worthy of investigation. In particular, while the very slow kinetics of the natural process are not practical for CO_2 storage and conversion purpose, the activation by mechanical treatment of olivine in the presence of H_2O and CO_2 has been demonstrated to be efficient to promote both the solid phases evolution and the gas-phase synthesis of light hydrocarbons, in particular of methane. The formation of carbonate solid phases and the methanation reaction, displayed faster kinetics compared to the hydrothermally activated ones and similar or higher conversion data. The whole pattern of physical and chemical transformations activated by mechanical treatment requires further deepening, but the results allowed to clarify some mechanistic aspects and suggested a possible line of future investigation. This process promoted H_2O dissociation with consequent H_2 formation, which in turn can promote FTT reactions over the mineral surface, and CO_2 hydrogenation rate can then increase, after an induction period related to CO_2 and H_2 activation, according to a sigmoidal trend often observed in

mechanochemical processes. Structural evolution of solid phases suggests the occurrence of a complex process that appears to be defined by the CO_2/H_2O ratio values. The presence of a "mechanochemical effect" is evident, i.e., the occurrence of an increased system reactivity specifically related to the activation by mechanical treatment.

The observed concentration values of methane and hydrocarbons may be influenced by the experimental set up: the analyses of the effects of parameters like the geometry reactor, as well as the milling dynamic parameter, i.e., frequency of collision, will be the focus of future work aimed at improving chemical results and deepening the knowledge of the whole process.

DATA AVAILABILITY STATEMENT

The datasets generated for this study are available on request to the corresponding author.

AUTHOR CONTRIBUTIONS

VF, FT, AT, and NG carried out the experimental activities: the several tests of CO_2 hydrogenation over olivine under mechanochemical treatment, the structural, thermal, and gaseous analyses. All of them collaborated with SE, SG, FG, and GM to analyse the different data. All authors discussed the results, wrote their respective parts of the manuscript, and revised the overall manuscript.

FUNDING

The present work is part of the CO2MPRISE, CO_2 absorbing Materials Project-RISE, a project that has received funding from the European Union's Horizon 2020 research and innovation programme, under the Marie Skłodowska-Curie, Grant Agreement No. 734873. This work has been partially supported also by RAS, Regione Autonoma Sardegna, through the project Sistemi innovativi di conversione di anidride carbonica a metano da fonti rinnovabili, under the program L.R.n.7/2007, call Capitale Umano ad Alta Qualificazione. The activity of VF was supported by a Ph.D. program in a collaborative scheme between the University of Sassari and Cagliari of Italy, which is especially endorsed by Autonomous Regional Administration of Sardinia (RAS).

ACKNOWLEDGMENTS

The authors acknowledge the support of the CeSAR UNISS, Centro Servizi di Ateneo per la Ricerca of the University of Sassari, for making available several instrumental techniques to carry out materials characterization.

REFERENCES

Ahmedabadi, P. M., and Kain, V. (2019). Modelling transformation kinetics of different solid-state reactions using sigmoidal model. *Materialia* 5:100235. doi: 10.1016/j.mtla.2019.100235

Baláž, P., Turianicová, E., Fabián, M., Kleiv, R. A., Briančin, J., and Obut, A. (2008). Structural changes in olivine (Mg, $Fe)_2SiO_4$ mechanically activated in high-energy mills. *Int. J. Miner. Process.* 88, 1–6. doi: 10.1016/j.minpro.2008.04.001

Bisbal, R., Gomez, F., Di Yorio, C., and Perez, M. (2015). Evaluación de las características y propiedades de fundición de Arena de Olivino Venezolana (Parte I). *Rev. la Fac. Ing. Univ. Cent. Venez.* 30, 95–110. Available online at: http://ve.scielo.org/scielo.php?script=sci_arttext&pid=S0798-40652015000300010

Cooper, C. (2009). A technical basis for carbon dioxide storage. *Energy Procedia* 1, 1727–1733. doi: 10.1016/j.egypro.2009.01.226

Cuéllar-Franca, R. M., and Azapagic, A. (2015). Carbon capture, storage and utilisation technologies: a critical analysis and comparison of their life cycle environmental impacts. *J. CO_2 Util.* 9, 82–102. doi: 10.1016/j.jcou.2014.12.001

Delogu, F., Mulas, G., Schiffini, L., and Cocco, G. (2004). Mechanical work and conversion degree in mechanically induced processes. *Mater. Sci. Eng. A* 382, 280–287. doi: 10.1016/j.msea.2004.05.047

Fabian, M., Shopska, M., Paneva, D., Kadinov, G., Kostova, N., Turianicová, E., et al. (2010). The influence of attrition milling on carbon dioxide sequestration on magnesium-iron silicate. *Miner. Eng.* 23, 616–620. doi: 10.1016/j.mineng.2010.02.006

Falkowski, P., Scholes, R. J., Boyle, E., Canadell, J., Canfield, D., Elser, J., et al. (2000). The global carbon cycle: a test of our knowledge of earth as a system. *Science* 290, 291–296. doi: 10.1126/science.290.5490.291

Fernández, A. I., Chimenos, J. M., Segarra, M., Fernández, M. A., and Espiell, F. (2000). Procedure to obtain hydromagnesite from a MgO-containing residue. *Kinet. Stud. Ind. Eng. Chem. Res.* 39, 3653–3658. doi: 10.1021/ie0003180

Furre, A. K., Eiken, O., Alnes, H., Vevatne, J. N., and Kiær, A. F. (2017). 20 Years of monitoring CO_2-injection at Sleipner. *Energy Procedia* 114, 3916–3026. doi: 10.1016/j.egypro.2017.03.1523

Giammar, D. E., Bruant, R. G. Jr., and Peters, C. A. (2005). Forsterite dissolution and magnesite precipitation at conditions relevant for deep saline aquifer storage and sequestration of carbon dioxide. *Chem. Geol.* 217, 257–276. doi: 10.1016/j.chemgeo.2004.12.013

Hänchen, M., Prigiobbe, V., Baciocchi, R., and Mazzotti, M. (2008). Precipitation in the Mg-carbonate system-effects of temperature and CO_2 pressure. *Chem. Eng. Sci.* 63, 1012–1028. doi: 10.1016/j.ces.2007.09.052

Hertwich, E. G., Aaberg, M., Singh, B., and Strømman, A. H. (2008). Life-cycle assessment of carbon dioxide capture for enhanced oil recovery. *Chin. J. Chem. Eng.* 16, 343–353. doi: 10.1016/S1004-9541(08)60085-3

Holm, N. G., Oze, C., Mousis, O., Waite, J. H., and Guilbert-Lepoutre, A. (2015). Serpentinization and the formation of H_2 and CH_4 on Celestial Bodies (Planets, Moons, Comets). *Astrobiology* 15, 587–600. doi: 10.1089/ast.2014.1188

Jones, L. C., Rosenbauer, R., Goldsmith, J. I., and Oze, C. (2010). Carbonate control of H_2 and CH_4 production in serpentinization systems at elevated P-Ts. *Geophys. Res. Lett.* 37:L14306. doi: 10.1029/2010GL043769

Klein, F. (2014). Magnetite in seafloor serpentinite-some like it hot. *Geology* 42, 135–138. doi: 10.1130/G35068.1

Kleiv, R. A., and Thornhill, M. (2006). Mechanical activation of olivine. *Miner. Eng.* 19, 340–347. doi: 10.1016/j.mineng.2005.08.008

Kloprogge, J. T., Martens, W. N., Nothdurft, L., Duong, L. V., and Webb, G. E. (2003). Low temperature synthesis and characterisation of nesquehonite. *J. Mater. Sci. Lett.* 22, 825–829. doi: 10.1023/A:1023916326626

Koukouzas, N., Gemeni, V., and Ziock, H. J. (2009). Sequestration of CO_2 in magnesium silicates, in Western Macedonia, Greece. *Int. J. Miner. Process.* 93, 179–186. doi: 10.1016/j.minpro.2009.07.013

Leung, D. Y. C., Caramanna, G., and Maroto-Valer, M. M. (2014). An overview of current status of carbon dioxide capture and storage technologies. *Renewable Sus. Energy Rev.* 39, 426–443. doi: 10.1016/j.rser.2014.07.093

Li, J. J., and Hitch, M. (2015). Ultra-fine grinding and mechanical activation of mine waste rock using a high-speed stirred mill for mineral carbonation.

Int. J. Miner. Metall. Mater. 22, 1005–1016. doi: 10.1007/s12613-015-1162-3

Markewitz, P., Kuckshinrichs, W., Leitner, W., Linssen, J., Zapp, P., Bongartz, R., et al. (2012). Worldwide innovations in the development of carbon capture technologies and the utilization of CO_2. *Energy Environ. Sci.* 5, 7281–7305. doi: 10.1039/c2ee03403d

Maroto-Valer, M. M., Fauth, D. J., Kuchta, M. E., Zhang, Y., and Andrésen, J. M. (2005). Activation of magnesium rich minerals as carbonation feedstock materials for CO_2 sequestration. *Fuel Process. Technol.* 86, 1627–1645. doi: 10.1016/j.fuproc.2005.01.017

McCollom, T. M., and Bach, W. (2009). Thermodynamic constraints on hydrogen generation during serpentinization of ultramafic rocks. *Geochim. Cosmochim. Acta* 73, 856–875. doi: 10.1016/j.gca.2008.10.032

Metz, B., Davidson, O., de Coninck, H., Loos, M., and Meyer, L. (2005). *IPCC, 2005: IPCC Special Report on Carbon Dioxide Capture and Storage.* Montreal, QC: MRS Bulletin.

Nagashima, S., Miyagawa, T., Matsumoto, M., Suzuki, S., Komaki, H., Takagi, M., et al. (2011). Life cycle assessment performed on a CCS model case in Japan and evaluation of improvement facilitated by heat integration. *Energy Procedia* 4, 2457–2464. doi: 10.1016/j.egypro.2011.02.140

Neubeck, A., Duc, N. T., Bastviken, D., Crill, P., and Holm, N. G. (2011). Formation of H_2 and CH_4 by weathering of olivine at temperatures between 30 and 70°C. *Geochem. Trans.* 12, 1–10. doi: 10.1186/1467-4866-12-6

Oelkers, E. H., Gislason, S. R., and Matter, J. (2008). Mineral carbonation of CO_2. *Elements* 4, 333–337. doi: 10.2113/gselements.4.5.333

Pehnt, M., and Henkel, J. (2009). Life cycle assessment of carbon dioxide capture and storage from lignite power plants. *Int. J. Greenhouse Gas Control* 3, 49–66. doi: 10.1016/j.ijggc.2008.07.001

Power, I. M., Wilson, S. A., and Dipple, G. M. (2013). Serpentinite carbonation for CO_2 sequestration. *Elements* 9, 115–121. doi: 10.2113/gselements.9.2.115

Rigopoulos, I., Petallidou, K. C., Vasiliades, M. A., Delimitis, A., Ioannou, I., Efstathiou, A. M., et al. (2015). Carbon dioxide storage in olivine basalts: effect of ball milling process. *Powder Technol.* 273, 220–229. doi: 10.1016/j.powtec.2014.12.046

Rigopoulos, I., Vasiliades, M. A., Ioannou, I., Efstathiou, A. M., Godelitsas, A., and Kyratsi, T. (2015). Enhancing the rate of *ex situ* mineral carbonation in dunites via ball milling. *Adv. Powder Technol.* 27, 360–371. doi: 10.1016/j.apt.2016.01.007

Sandvik, K. L., Kleiv, R. A., and Haug, T. A. (2011). Mechanically activated minerals as a sink for CO_2. *Adv. Powder Technol.* 22, 416–421. doi: 10.1016/j.apt.2010.06.004

Singh, B., Strømman, A. H., and Hertwich, E. G. (2011). Comparative life cycle environmental assessment of CCS technologies. *Int. J. Greenhouse Gas Control* 5, 911–921. doi: 10.1016/j.ijggc.2011.03.012

Stocker, T. F., Qin, D., Plattner, G.-K., Tignor, M., Allen, S. K., and Boschung, J. (eds.). (2014). "Climate change 2013: the physical science basis: Working Group," in *Fifth Assessment Report of the Intergovernmental Panel on Climate Change* (University of Bern), 5.

Stopic, S., Dertmann, C., Modolo, G., Kegler, P., Neumeier, S., Kremer, D., et al. (2018). Synthesis of magnesium carbonate via carbonation under high pressure in an autoclave. *Metals* 8:993. doi: 10.3390/met8120993

Styring, P., and Jansen, D. (2011). *Carbon Capture and Utilisation in the Green Economy*. Centre for Low Carbon Futures.

Turianicová, E., and Baláz, P. (2008). "A possible way to storage carbon dioxide on mechanically activated olivine (Mg, $Fe)_2SiO_4$," in *VI International Conference on Mechanochemistry and Mechanical Alloying* (Jamshedpur), 316–319.

Turianicová, E., Baláž, P., Tuček, L., Zorkovská, A., Zelenák, V., Németh, Z., et al. (2013). A comparison of the reactivity of activated and non-activated olivine with CO_2. *Int. J. Miner. Process.* 123, 73–77. doi: 10.1016/j.minpro.2013.05.006

Von Der Assen, N., Jung, J., and Bardow, A. (2013). Life-cycle assessment of carbon dioxide capture and utilization: avoiding the pitfalls. *Energy Environ. Sci.* 6, 2721–2734. doi: 10.1039/c3ee41151f

Weisser, D. (2007). A guide to life-cycle greenhouse gas (GHG) emissions from electric supply technologies. *Energy* 32, 1543–1559. doi: 10.1016/j.energy.2007.01.008

Young, R. A. (1993). *The Rietveld Method*. Atlanta, GA: Oxford University Press.

Zapp, P., Schreiber, A., Marx, J., Haines, M., Hake, J.-F., and Gale, J. (2012). Overall environmental impacts of CCS technologies-a life cycle approach. *Int. J. Greenhouse Gas Control* 8, 12–21. doi: 10.1016/j.ijggc.2012.01.014

Zhang, P., Anderson, H. L., Kelly, J. W., Krumhansl, J. L., and Papenguth, H. W. (2000). Kinetics and mechanisms of formation of magnesite from hydromagnesite in brine. *Appl. Geochem.* 286, 1748–1753. Available online at: https://www.osti.gov/servlets/purl/764025

Conflict of Interest: The authors declare that the research was conducted in the absence of any commercial or financial relationships that could be construed as a potential conflict of interest.